JCS ePress online publication date 28 March 2006

N-terminal palmitoylation within the appropriate amino acid environment conveys on NOS2 the ability to progress along the intracellular sorting pathways

Inmaculada Navarro-Lérida[1], Alberto Álvarez-Barrientos[2] and Ignacio Rodríguez-Crespo[1,*]

[1]Departamento de Bioquímica y Biología Molecular, Facultad de Ciencias Químicas, Universidad Complutense de Madrid, 28040 Madrid, Spain
[2]Unidad de Citometría, Fundación CNIC, Instituto de Salud Carlos III, Melchor Fernández Almagro 3, 28040 Madrid, Spain
*Author for correspondence (e-mail: nacho@bbm1.ucm.es)

Accepted 5 January 2006
Journal of Cell Science 119, 1558-1569 Published by The Company of Biologists 2006
doi:10.1242/jcs.02878

Summary

We have analysed the mechanism by which palmitoylation permits the progression of nitric oxide synthase 2 (NOS2) along the ER-Golgi-TGN pathway. Introduction of an additional myristoylation site at the N-terminus of NOS2 resulted in a chimera that displayed an enhanced association with the particulate fraction and with the plasma membrane but did not display increased enzymatic activity. In the absence of palmitoylation, introduction of a surrogate myristoylation site resulted in a mutant NOS2 with only 25% activity compared with the wild-type enzyme. Hence, the novel surrogate myristoyl moiety not only failed to increase NOS2 activity when introduced in a wild-type sequence environment, but was also unable to rescue the inactive phenotype of the Cys3Ser mutant. Introduction of an additional palmitoylatable Cys at position 2 of the wild-type sequence resulted in a chimera that associated to a larger degree with membranes and displayed decreased activity. Our data indicate that palmitoylation of inducible NOS at position 3 exquisitely determines its transit along the secretory pathway following a route that cannot be mimicked by a surrogate myristoylation or by a palmitate at position 2. In addition, the exit of NOS2 from the TGN and the accumulation in the cellular plasma membrane per se did not correlate with increased ·NO synthesis.

Supplementary material available online at
http://jcs.biologists.org/cgi/content/full/119/8/1558/DC1

Key words: NOS2, Palmitoylation, Caveolae, Nitric oxide

Introduction

In fundamental cell biological processes such as signal transduction, enzymatic activity or intracellular fusion during vesicular transport, a large number of proteins are recruited to and released from the cytoplasmic surface of intracellular membranes (Casey et al., 1995; Rothman and Orci, 1992). In order to perform their functions at the correct time and place, some proteins must rely on regulated processes guiding their binding to or their release from the membrane lipid bilayer (James and Olson, 1990; Resh, 1999). In this regard, modification with lipophilic moieties has been described as an important mechanism involved in membrane anchoring of cytoplasmic proteins, which tightly regulates their proper intracellular targeting (Gonzalo and Linder, 1998; Smotrys and Linder, 2004). Protein fatty acylation includes different types of fatty acids, such as myristate and palmitate, or isoprenylation with farnesyl or geranylgeranyl moieties (Zhang and Casey, 1996; Magee and Seabra, 2003; Dietrich and Ungermann, 2004).

Among the three human nitric oxide synthase (NOS) isoforms that have been cloned and characterised, both NOS2 (inducible NOS) and NOS3 (endothelial NOS) are known to become palmitoylated. In fact, the N-terminus of NOS3 is irreversibly myristoylated at Gly2 and reversibly palmitoylated at Cys15 and 26 in a well-known process responsible exclusively for its targeting to caveolae (Liu et al., 1997; Feron et al., 1998 and references therein). On the other hand, NOS2 is only modified by palmitic acid at Cys3 when both the basic residues Lys6 and Lys10 together with the hydrophobic residue Pro4 are present (Navarro-Lérida et al., 2004a). When the palmitoylated Cys3 residue is substituted with Ser, the mutant NOS2 becomes misfolded, aggregates with intracellular membranes and does not progress along the secretory pathway. Shortly after we described the N-terminal palmitoylation of NOS2, the palmitoylation of the human Kv1.1 channel was also reported (Gubitosi-Klug et al., 2005) highlighting certain similarities in the sequences that become palmitoylated among NOS2 (ACPWKFLFK), Kv1.1 channel (ACPSKTDFF), CD36 (ACRSKTIK) and the cation-dependent mannose-6-phosphate receptor (VCRSKPRNV). It is tempting to speculate that, inside the cell, these proteins and some others not yet identified might be the substrates of the same palmitoyl transferase. This sequence motif includes an Ala or Val residue at the –1 position (considering the palmitoylatable Cys residue as 0), an uncharged residue at +2 with the capacity to make hydrogen bonds (Trp or Ser) and preferentially a Lys residue at the +3 position.

We have now addressed the mechanism by which palmitoylation allows the proper transit of NOS2 along the secretory pathway. In this work we have tried to gain further

understanding of the reasons that underlie NOS2 palmitoylation and its differences with the subcellular targeting of NOS3 which becomes irreversibly and enzymatically myristoylated at Gly2 and doubly palmitoylated at the side chains of Cys15 and Cys26. This latter modification can be modulated, hence determining the translocation of the enzyme to caveolae/rafts and its inhibitory association with the caveolin molecule in endothelial cells. Incubation of both recombinant NOS2 or NOS3 with the 'scaffolding domain' peptide of both caveolin-1 (residues 82-101) and caveolin-3 (residues 55-74) completely abrogated nitric oxide synthesis (García-Cardena et al., 1997), an observation that might suggest that within the cell, the activity of these enzymes must be modulated through its interaction with caveolin. However, in contrast to NOS3, the palmitoylation of NOS2 does not result in its translocation to caveolar domains (Navarro-Lérida et al., 2004a). Indeed, NOS2 can become associated with caveolin-1 (and marginally to caveolin-2 and -3) within muscle cells and this interaction is inhibitory for the enzyme. Interestingly, in mature myotubes, the same cytokine stimuli that induce NOS2 expression lead to the downregulation of caveolin-1 levels, hence allowing NOS2 to reach its full activity (Navarro-Lérida et al., 2004b).

With this in mind, we have created a number of NOS2 chimeras that could allow us to inspect the functionality of NOS2 palmitoylation. Some of our constructs result in non-acylated, myristoylated, palmitoylated or doubly acylated proteins. Sorting along the secretory pathway was analysed using the drugs brefeldin A, monensin and megalomicin. Our main conclusion is that palmitoylation of NOS2 at Cys3 determines exquisitely its correct exit from the Golgi en route through the plasma membrane as well as its ·NO-synthesising activity. Neither myristoylation at Gly2, nor dual palmitoylation at Cys2 and Cys3 could substitute for palmitoylation at Cys3 in terms of protein activation along the secretory pathway. Apparently, each of the surrogate post-translational lipidic modification conferred NOS2 with an erroneous subcellular sorting route resulting in diminished enzymatic activity.

Results

Construction of NOS2 chimeras, enzymatic activity and radiolabeling with myristic and palmitic acids

Endothelial NOS (NOS3) becomes N-terminally myristoylated and, when subsequently palmitoylated at positions Cys15 and Cys26 becomes targeted to caveolae (Liu et al., 1997; Feron et al., 1998). Myristoylation is a prerequisite for protein palmitoylation mimicking the well-known dependence of S-acylation on prior membrane association via myristoyl, prenyl or transmembrane peptide moieties (Milligan et al., 1995; Dunphy and Linder, 1998; McCabe and Berthiaume, 1999). However, we have observed that NOS2 is palmitoylated at Cys3 without the presence of any other lipid modification (Navarro-Lérida et al., 2004a). With that in mind, we investigated whether a surrogate myristoylation site in the NOS2 sequence could render a protein with similar characteristics to endothelial NOS. First of all, using wild-type NOS2 as template, we created different mutants at the N-terminus of the polypeptide sequence (Fig. 1A). In the first mutant, Cys3 was changed to Ser (C3S NOS2-GFP); the second mutant contains a myristoylation consensus sequence at Gly2 and Ser6 (Myr-NOS2-GFP); the third is a double mutant, containing the myristoylation site of Myr-NOS2-GFP together with the Cys3 to Ser mutation (Myr/C3S NOS2-GFP); the fourth mutant combines the mutations of the third mutant with an additional palmitoylatable Cys2 (A2C NOS2-GFP). Since we can measure the amount of nitric oxide released to the medium in the form of nitrites, we determined the enzymatic products of the conversion of L-Arg into citrulline plus ·NO by wild-type NOS2 as well as its mutant

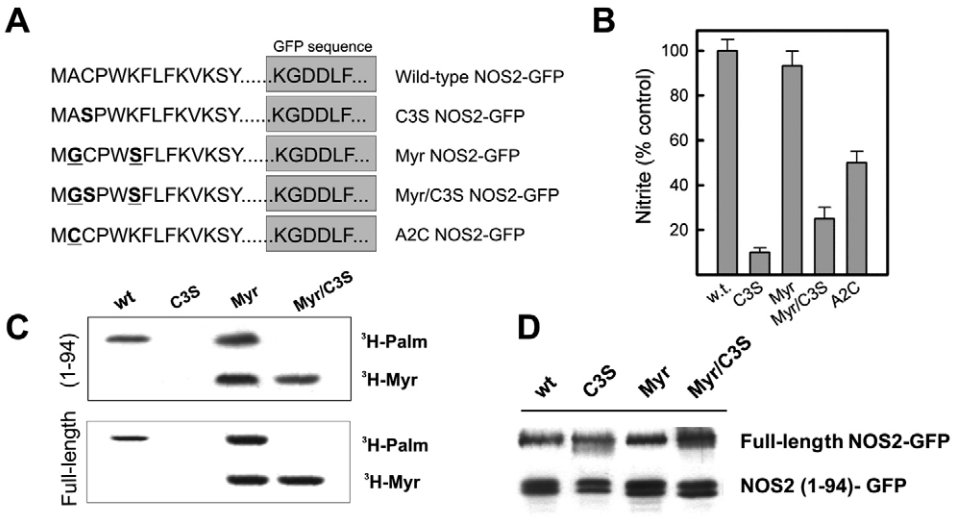

Fig. 1. Wild-type and mutant NOS2-GFP chimeras. (A) The N-terminus of NOS2 was mutated by PCR, creating C3S, Myr, Myr/C3S and A2C mutant chimeras fused to GFP. We created both full-length NOS2 chimeras (residues 1-1144) and short chimeras (residues 1-94). The different NOS2-GFP constructs were inserted into a pCDNA3 vector that was used to transfect COS7 cells and the enzymatic activity (B), incorporation of radioactive palmitate and myristate (C) and protein expression (D) were determined. Enzymatic activity of NOS2 was determined using the Griess method as previously reported (Navarro-Lérida et al., 2004). Transfected COS7 cells were starved for 1 hour in DMEM without serum and were then metabolically labelled for 4 hours with either [^{3}H]myristic acid (Myr) or [^{3}H]palmitic acid (Palm). Cell lysate proteins were separated by SDS-PAGE and expression of the NOS2 chimeras was determined by western blotting with antibodies to GFF.

chimeras (Fig. 1B). As previously shown (Navarro-Lérida et al., 2004a), the mutant chimera where the palmitoylatable Cys3 was substituted with Ser practically lacked enzymatic activity. Introduction of a myristoyl tag at the N-terminus rendered a mutant protein with very similar activity rate when compared with the wild-type phenotype. Remarkably, in the absence of palmitoylation, myristoylation alone (Myr/C3S chimera) was unable to match the wild-type proteins in terms of catalysis, displaying ~27% of wild-type NO-synthesising activity. Somewhat surprisingly, two consecutive palmitoylatable Cys residues also produced a chimera with reduced activity, displaying 50% activity when compared with the wild-type protein (Fig. 1B).

To inspect the targeting signals contained within the N-terminus per se, every construct was obtained as a full-length NOS2-GFP chimera and as a NOS2 (1-94 amino acid) GFP chimera, the latter lacking the caveolin-1-interacting motif. Metabolic radiolabelling of the full-length and (1-94)-GFP constructs was performed using [9,10-^{3}H]-myristic acid or [9,10-^{3}H]-palmitic acid followed by immunoprecipitation of the cell lysates with the anti-GFP antibody (Fig. 1C). Only GFP chimeras that possessed the N-terminal Gly in the context of a consensus myristoylation sequence (Ser6) incorporated myristic acid (Myr, and Myr/C3-GFP) resulting in the efficient incorporation of palmitic acid in the wild-type NOS2 and Myr NOS2-GFP constructs. Remarkably, the myristoylated and palmitoylated mutant showed a higher level of incorporation of palmitate than its wild-type NOS2 counterpart. As expected, transient transfection of COS7 cells with the different pCDNA plasmids containing the chimeric GFP cDNAs resulted in similar levels of expression for all the recombinant proteins (Fig. 1D). The doublet observed in the case of the 1-94 GFP chimeras is indicative of a certain degree of proteolysis observed for these constructs (see below).

Immunofluorescence of the NOS2 chimeras and colocalisation with the Golgi apparatus marker β-cop

To examine the subcellular expression patterns of each mutant, plasmids encoding GFP-tagged wild-type NOS2, C3S NOS2, Myr NOS2 and Myr/C3S NOS2 were transfected in COS7 cells and examined by confocal microscopy (Fig. 2). Immunofluorescence data indicated that all the full-length chimeras were excluded from the cell nucleus and associated with perinuclear or plasma membrane areas to a different extent. Interestingly, introduction of a surrogate myristoylation site produced a mutant protein that associated with the plasma membrane to a greater degree when compared with the wild-type NOS2 distribution (Fig. 2A). Probably this plasma membrane enrichment of the myristoylated and palmitoylated mutant is related to the difference in the level of incorporation of palmitate shown between the Myr NOS2 mutant and the wild-type NOS2 because some palmitoyltransferase activities are known to become enriched in the plasma membrane (Dunphy et al., 1996; Bijlmakers and Marsh, 2003). Mutation of the Cys3 to Ser in NOS2 created a recombinant chimera that accumulated to cis-Golgi areas (Navarro-Lérida et al., 2004a). However, introduction of a novel myristoyl moiety (Myr/C3S mutant) was unable to recover the phenotype of the wild-type NOS2, although it conferred important changes on C3S NOS2 distribution. In fact, the myristoylated and non-palmitoylated chimera changed the cis-Golgi accumulation into a multiple intracellular membrane localisation, (including the nuclear envelope) and an enrichment in perinuclear areas showing a partially cytoplasmic distribution in the cell. However, in the absence of palmitoylation, no plasma membrane staining could be observed.

To elucidate the role of the N-terminal end in the absence of interference from the caveolin-binding motif (FPAPFNGW) that is found spanning residues 358-366, we created deletional chimeras of NOS2-GFP containing only the first 94 amino acids of NOS2 fused to GFP (Fig. 2B). These constructs would presumably localise to certain subcellular regions dictated only by the acylation state of the N-terminus. Unlike the full-length chimeras, the wild-type and the C3S NOS2(1-94) chimeras displayed partial nuclear staining. On the other hand, the myristoylated and palmitoylated mutant Myr NOS2(1-94) and the mutant exclusively modified by myristic acid were excluded from the nucleus (Fig. 2B). The presence of both lipid moieties confers to the Myr NOS2(1-94) mutant a practically exclusive plasma membrane localisation and a focal perinuclear staining. This phenotype contrasts with the subcellular distribution of the Myr/C3S mutant where the elimination of the putative palmitoylation site Cys3 introducing a myristoylation site results in a distribution characterised by the nuclear exclusion and the completely loss of plasma membrane staining, with an enrichment in intracellular membrane as well as in the ER. This clearly resembles the phenotype shown by the Myr NOS2 mutant when treated with 2-Br-palmitate (Fig. 2C). Since we wanted to determine whether the perinuclear staining of the NOS2(1-94) chimeras corresponded with Golgi network labelling, double immunofluorescence was performed with the Golgi marker β-cop (Fig. 2D). We compared the subcellular distribution of a myristoylated plus palmitoylated (Myr), a myristoylated (Myr/C3S) and a doubly palmitoylated (A2C) NOS2(1-94) chimera with myristoylated plus palmitoylated endothelial NOS chimeras known to be enriched in rafts (Navarro-Lérida et al., 2002). In all four cases the staining observed in perinuclear areas corresponded to the Golgi network, as indicated by the β-cop colocalisation. However, the subcellular distribution was different in all cases. Whereas the Myr/C3S chimera displayed a distribution that indicated that upon exiting the Golgi it associated with other intracellular vesicles, both the dually palmitoylated A2C and the dually acylated Myr NOS2(1-94) chimeras showed clear Golgi and plasma membrane staining with no traces of label in TGN or intracellular vesicles. The dual Golgi-plasma membrane immunofluorescence is especially apparent in the case of the Myr NOS(1-94) chimera. However, NOS3, which becomes myristoylated and palmitoylated does localise to the Golgi, TGN and partially in the plasma membrane (Fig. 2D, bottom row).

Membrane partitioning, enrichment in DRMs and colocalisation with caveolin-1

To investigate the effect of the various acylation states on the membrane partitioning of the full length or (1-94) GFP chimeras, we fractionated cellular lysates containing identical amounts of each chimera into supernatant (S-soluble) and pellet (P-membrane associated) fractions after ultracentrifugation at 200,000 ***g*** (Fig. 3A). The palmitoylated wild-type full length NOS2 transfected in COS7 was found both in the soluble and particulate fractions (in an approximate ratio of 40:60) whereas the myristoylated plus palmitoylated

Myr-NOS2 GFP or a mutant of NOS2 where an additional palmitoylatable Cys residue was introduced at position 2 (dually palmitoylated mutant A2C NOS2-GFP) were associated with the membrane fraction to >80%. Myristoylated but not palmitoylated (Myr/C3S-GFP) was found distributed in both fractions, but the majority (at least ~60% on average) was found in the soluble fraction (Fig. 3A). In this case, N-terminal myristoylation increased the overall hydrophobicity of the engineered GFP chimeras resulting in an increased association with cellular membranes, specially in the case of the Myr NOS2-GFP mutant where the dual acylation leads to a practically 100% of fractionation into pellet. In the case of the short chimeras, introduction of any additional acyl chain also resulted in increased association with the particulate fraction of the cells (Fig. 3A, right plot).

We next analysed the targeting of the various acylated constructs of NOS2 to the Triton-X100-insoluble membranes (DRMs) preparing 40:30:5% sucrose discontinuous gradients in the presence of the detergent following a well-defined procedure of caveolae extraction (Lisanti et al., 1999). The majority of both the full-length and (1-94) wild-type NOS2 appeared in the high-density fractions (at the bottom of the tube) and a very limited amount of protein co-fractionated with DRMs (Fig. 3A). In fact, association with DRMs resulted in proteolytic degradation by the proteasome (Felley-Bosco et al., 2000; Navarro-Lérida et al., 2004b). In contrast to the expected results, only a very limited amount of the full-length and (1-94) Myr NOS2 chimeras were observed in DRMs: this was most of the immunodetected protein associated with the Triton X-100-soluble fractions at the bottom of the tube. These data contrast with the distribution of the short Myr NOS2-GFP and, to a lesser extent, the full-length construct in the plasma membrane. In the absence of palmitoylation, myristoylation alone seemed to be unable to target either the full-length or the (1-94) Myr/C3S NOS2 chimeras to DRMs. Nevertheless, dual palmitoylation resulted in a significant enrichment of A2C NOS2 in DRMs, both in the full-length construct and its short counterpart. In any case, translocation to DRMs detected in our positive control of caveolar targeting linker-$(SAG)_9$-GFP (Navarro-Lérida et al., 2002) was not attained by any of the

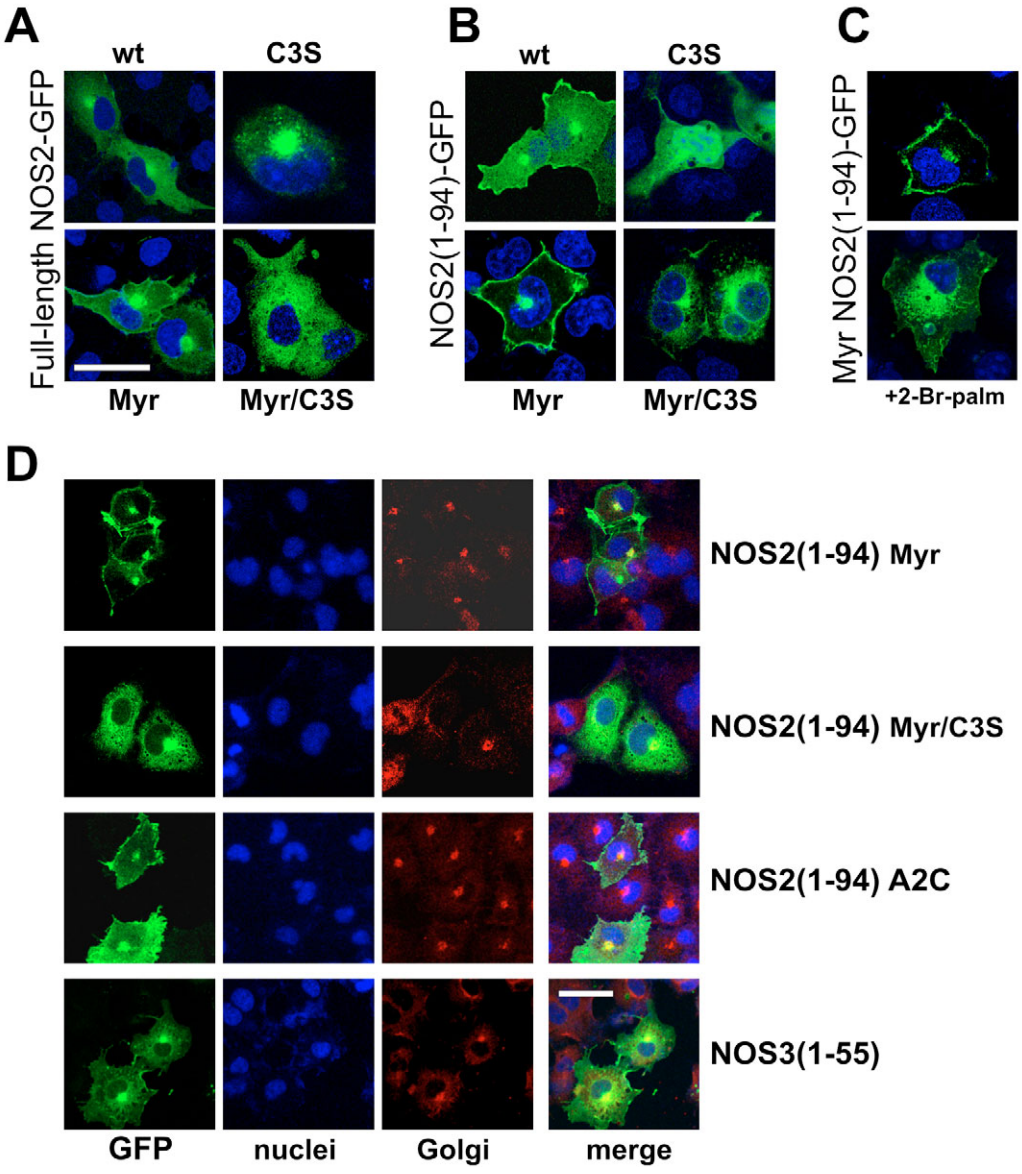

Fig. 2. Subcellular localisation of the various constructs and laser confocal microscopy with the Golgi marker β-cop. COS7 cells were transfected with the various NOS2-GFP constructs and the fluorescence was analysed 36 hours post transfection. The subcellular localisation of the full-length NOS2-GFP chimeras (A) and the (1-94)-NOS2 chimeras (B) was determined. Changes induced in the subcellular distribution of the Myr chimera when treated with 10 μM 2-Br-Palmitate were also determined (C). In order to determine the colocalisation of the Myr, Myr/C3S and A2C NOS2(1-94) chimeras with the Golgi marker β-cop, double immunofluorescence staining was performed using a Cy3-conjugated secondary antibody. As a positive control, we used residues 1-55 of NOS3 fused to GFP, which is known to become myristoylated and palmitoylated (Navarro-Lérida et al., 2002). Cell nuclei were stained with Hoechst 33258 (blue). Bars, 50 μm.

NOS2 constructs. When we tried to correlate the flotation experiments with the double staining with caveolin-1 antibodies we concluded that the plasma membrane immunolocalisation displayed by caveolin-1 in COS7 cells stained areas that were also positive for three of our chimeras: Myr, Myr(1-94) and A2C (1-94) (Fig. 3B). We determined that 10% of the Myr full-length GFP fluorescence colocalised with caveolin-1, 32% in the case of the Myr(1-94) chimera and 11% in the case of the A2C chimera. In consequence, the colocalisation of our NOS2-GFP chimeras with caveolin-1 in the plasma membrane does not fully correlate with DRM enrichment detected by Triton X-100 sucrose gradients. This

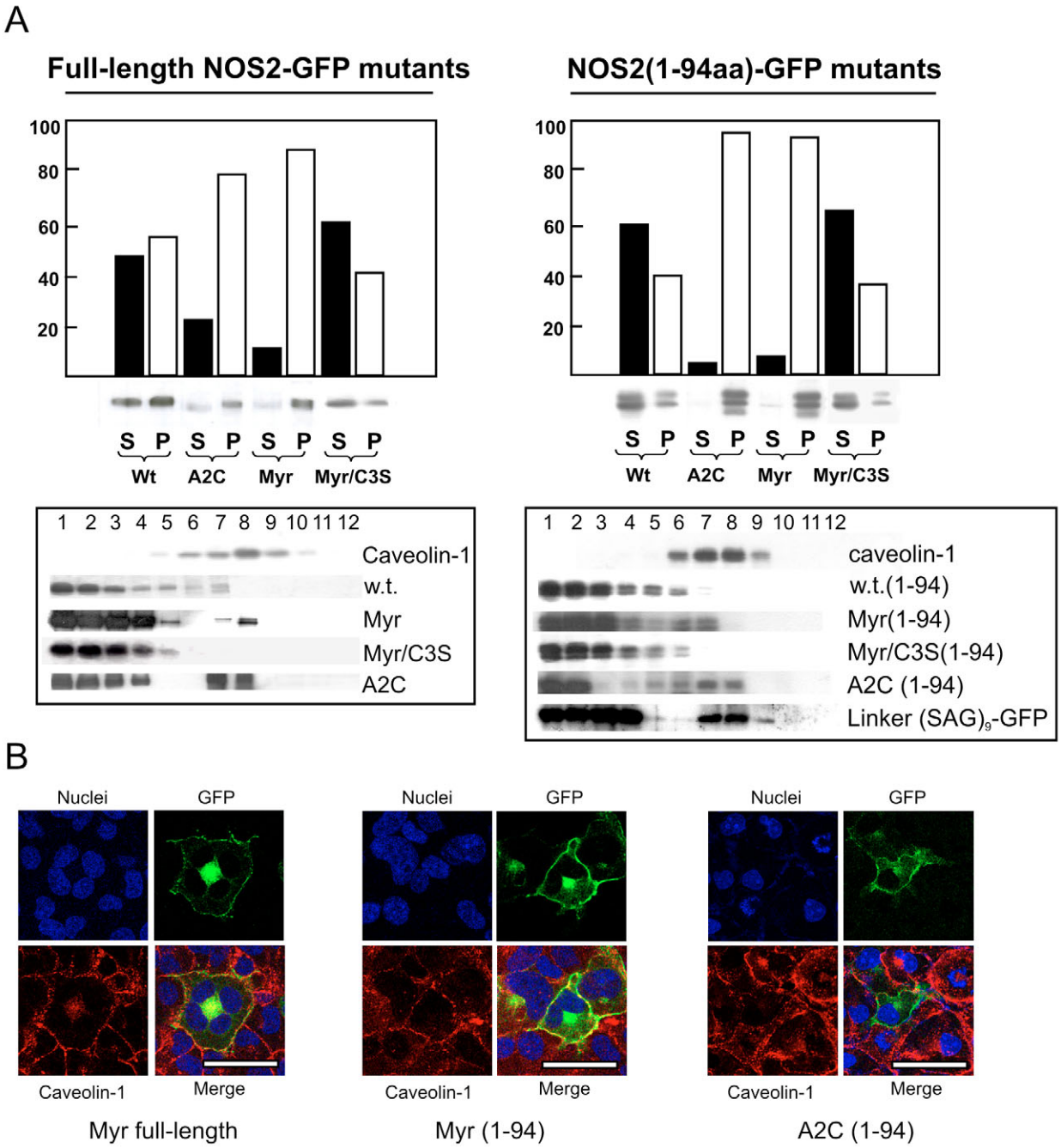

Fig. 3. Subcellular fractionation of COS7 cells expressing the various GFP constructs. (A) Transfected COS7 were lysed and after clarification of the cellular debris by centrifugation, fractionated into supernatant (S) and pellet (P) fractions by ultracentrifugation for 16 hours at 200,000 ***g*** as described in the Materials and Methods section. The fractions were subjected to a SDS-PAGE, analysed by western blot with an antibody against GFP and the resulting bands were quantified using UVIband V97 software. In addition, COS7 cells transfected with the tagged GFP constructs were extracted in the presence of Triton X-100 at 4°C and subjected to centrifugation on a 40:30:5% sucrose gradient. After centrifugation, the gradient tubes were divided into 12 equal aliquots collected from the bottom and analysed by SDS-PAGE and western blot (lower panels). (B) COS7 cells were transfected with the Myr, Myr (1-94) and A2C (1-94) NOS2-GFP. The bottom right panels are the merges of the three fluorescence signals. Bars, 50 μm.

led us to conclude that plasma membrane immunofluorescence did not necessarily correspond with caveolae enrichment, despite the coincidence with caveolin-1 labeling.

Different kinetics of wild-type, Myr and A2C NOS2(1-94) distribution in COS7 cells

At this point we evaluated the intrinsic differences conferred by either a palmitoyl or a myristoyl moiety located at the N-terminus of NOS2 in terms of transit along the secretory route. Modulation of different exocytic steps at a low temperature (25°C) corroborated the fact that wild-type NOS2 and Myr NOS2-GFP followed distinct routes towards the plasma membrane. Since the fusion of the cis-, medial- and trans-Golgi cisternae necessary for protein sorting is a temperature-dependent process, a further experiment was performed in which 8 hours after transfection at 37°C, the COS7 cells were transferred into a CO_2 incubator maintained at 25°C. Under conditions where identical amounts of protein were considered, the wild-type NOS2 was approximately 44% active when temperature of the cells had been lowered down to 25°C and the GFP fluorescence accumulated appreciably in areas adjacent to the cell nucleus (Fig. 4A). Both at 37°C and 25°C the mutant C3S NOS2 chimera displayed very low activity, concomitant with a clear perinuclear fluorescence. Finally, the myristoylated and palmitoylated mutant expressed at 25°C showed only a 20% decrease in its ·NO synthesising activity when compared with the rates at 37°C, with no significant changes in its cellular distribution (Fig. 4A, right panel). It is

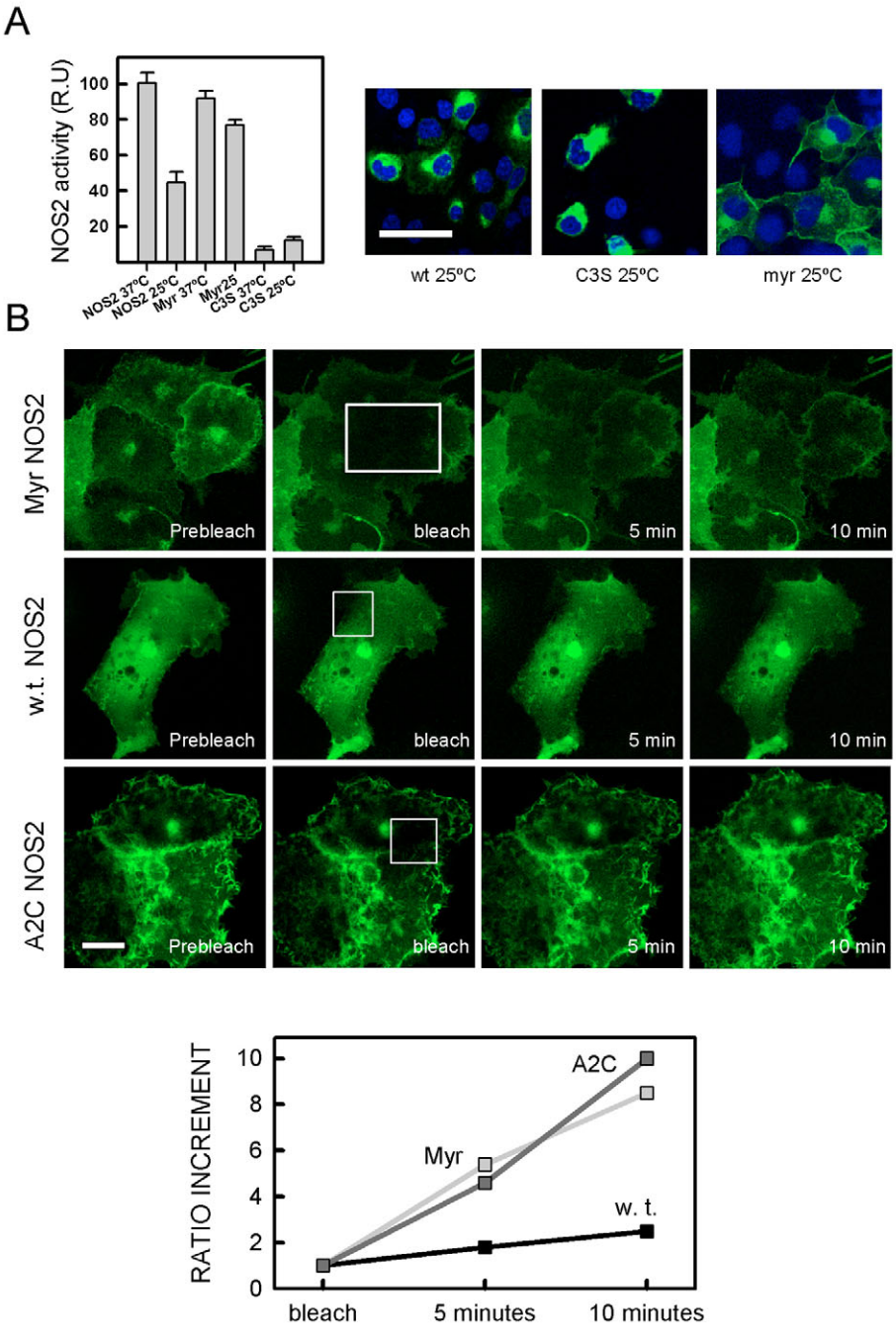

Fig. 4. Nitric oxide synthesis, subcellular targeting of the NOS2 chimeras at 25°C and in vivo recovery of the subcellular localisation of the wild-type and Myr NOS2 chimeras. (A) COS7 cells were transfected with the wild-type, Myr and C3S NOS2 chimeras and the cells were grown at both 37°C and 25°C. The NOS2 activity was determined at both temperatures using the Griess assay and was represented relative to the wild-type (relative units, RU) at 37°C (usually about 20 μM nitrites). At the same time, the cells grown at 25°C were fixed and analysed by laser confocal microscopy following the GFP fluorescence after excitation at 488 nm. (B) Areas in the plasma membrane with positive fluorescence for GFP (boxed) were selected in the wild-type, Myr (1-94) and A2C(1-94) NOS2 chimeras. The green fluorescence was bleached with the laser and the cell was allowed to recover the plasma membrane fluorescence for 30 minutes. The recovery is representative of three independent experiments. The ratio increment is depicted below. Bar, 50 μm.

particularly noticeable that the Myr NOS2 chimera could still display plasma membrane immunofluorescence even in cells grown at 25°C.

Fig. 4B shows the fluorescence recovery in the plasma membrane of wild-type NOS2(1-94), Myr NOS2(1-94) and A2C NOS2(1-94) after photobleaching with the laser beam. For photobleach experiments, an area of plasma membrane GFP was bleached using the 488 nm laser line and the recovery was monitored scanning once every 30 seconds for 30 minutes. The velocity of recovery of the plasma membrane staining was three to four times faster in the case of the myristoylated and A2C singly palmitoylated mutant compared with the wild-type NOS2, suggesting that the secretory pathways followed by the double acylated mutants (either myr-palm or palm-palm) are different from the wild-type NOS2 (Fig. 4B). In fact, after 10 minutes, only a very limited recovery was observed in the case of the wild type chimera (Fig. 4B bottom plot). Although we cannot rule out the possibility of a redistribution of fluorescently-tagged chimeras from other areas of the cell, our data suggest that myristoylation and double palmitoylation, in addition to contributing to the targeting of NOS2 to the plasma membrane, increases the speed of movement of NOS2 from the ER through the Golgi pool towards the plasma membrane.

Effect of nitric oxide on NOS2 progression along intracellular pathways

Nitric oxide is known to prevent addition of the palmitate moiety to certain neuronal proteins such as GAP43 and SNAP-25 hence restricting neuronal growth (Hess et al., 1993). Since, in theory, NOS2 could be responsible self-catalytically for the attachment-detachment of the palmitoyl moiety to its Cys3 residue we analysed the sites of intracellular synthesis of ·NO using the probe DAR, known to react with nitric oxide rendering a fluorescent precipitate that does not diffuse significantly (Fig. 5). At this point, it was conceivable that only the plasma-membrane-localised NOS2 might be active whereas the pool associated with the ER and Golgi apparatus lacks activity. Unexpectedly, all the intracellular NOS2 proved to possess ·NO-synthesising activity, as demonstrated by the DAR reactivity, that was practically coincident with the NOS2 immunofluorescence. A pixel-by-pixel analysis revealed that 92.8% of the DAR red fluorescence colocalised with the NOS2-GFP fluorescence. As expected, NOS2-negative cells displayed no synthesis of nitric oxide (Fig. 5A). Once we proved that the inducible nitric oxide was active in the cytosol of the cells we intended to ascertain if the availability of either the NOS2 substrate L-Arginine or the cofactor tetrahydrobiopterin were limiting its enzymatic activity, hence promoting the progression of NOS2 along the secretory pathway. Therefore, to examine the importance of the correct transit through the ER-Golgi trans-Golgi compartments to reach full activity of NOS2 en route to the plasma membrane, activity changes of wild-type NOS2, C3S or Myr NOS2 mutants were analysed after addition of extra L-Arginine (10 mM) and tetrahydrobiopterin (10 μM) to the medium (Fig. 5B). Curiously, the presence of both compounds in the medium concomitantly produced only a moderate increase in the activity of wild-type and Myr NOS2, whereas C3S NOS2 was not affected. This suggests that active NOS2, upon its exit from the Golgi apparatus reaches full activity when larger amounts of the cofactor tetrahydrobiopterin and the substrate L-arginine become available. In addition, the inability of the C3S mutant to synthesise nitric oxide must be due to its lack of palmitoylation, which could result in the inability to dimerise or in an incorrect transit, rather than the deficiency in substrate or cofactor. On the other hand, the addition of the NOS2 inhibitor 1400W or the ·NO donor DetaNONOate to the wild-type NOS2 did not alter its subcellular distribution: a fact that indicates that nitric oxide itself does not determine the intracellular transit of inducible nitric oxide synthase (Fig. 5C). Both in the absence of ·NO synthesis (with 1400W) or with excess ·NO, NOS2 was still able to partially reach the plasma membrane (see arrows in Fig. 5C). This suggests that the NOS2-generated nitric oxide is not responsible for reacting with the free thiol in the side chain of Cys3, hence inhibiting palmitoylation of its own N-terminus.

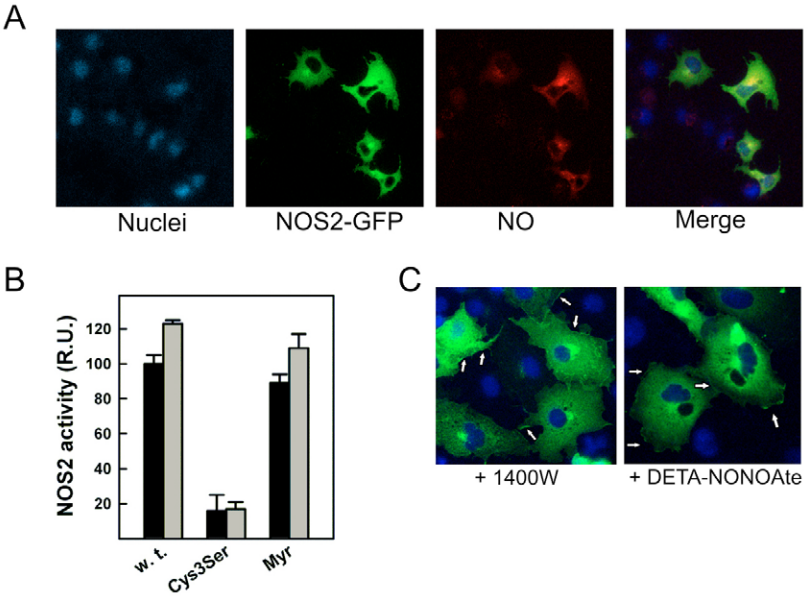

Fig. 5. Localisation of the sites of intracellular synthesis of ·NO in vivo, NOS2 activity in the presence of additional substrate and cofactor and effect of the NOS2 inhibitor 1400W and the ·NOS donor DETA-NONOate on the NOS2 fluorescence. (A) COS7 cells were transfected with the full-length wild-type NOS2-GFP and 36 hours post-transfection, the cells were incubated in vivo with 5 μM of the ·NO-sensitive probe diamino-Rhodamine-4M (DAR-4M) for 1 hour at 37°C. The location of the intracellular sites of ·NO synthesis is indicated in red. (B) COS7 cells transfected with the wild-type, C3S and Myr full-length NOS2-GFP chimeras were incubated with (shaded bars) or without (black bars) an excess of the NOS2 substrate L-Arg (10 mM) and the cofactor H_4B (10 μM) and ·NO-synthesising activity was determined. (C) Changes in the immunofluorescence signal of the wild-type full length NOS2-GFP chimera after addition of 100 μM of the NOS inhibitor 1400W or 100 μM of the ·NO donor DETA-NONOate. Arrows indicate the plasma membrane areas where the NOS2 GFP fluorescence can be observed. Cell nuclei were stained with Hoechst 33258 (blue).

Disruption of the secretory pathway by brefeldin A abrogates NOS2 palmitoylation

Maturation of newly synthesised NOS2 into the palmitoylated form requires the association of the soluble protein with a palmitoyl transferase. Because palmitoylation of proteins can occur during transit through the secretory pathway or at the plasma membrane (Bijlmakers and Marsh, 2003) we tested whether disruption of the secretory pathway in the different steps of the route towards the plasma membrane affected palmitoylation of wild-type NOS2. Brefeldin A treatment, which inactivates Arf 1, is known to lead to the dissociation of COP I and other peripheral proteins from the Golgi membrane, resulting in Golgi enzymes redistributing to the ER as the Golgi structure disassembles (Klausner et al., 1992). On the other hand, the ionophore monensin is commonly used to partially disrupt the integrity of the Golgi network and to inhibit vesicular transport in eukaryotic cells (Griffiths et al., 1983). Finally, megalomicin produces profound morphological and functional alterations on the Golgi complex of cultured cells causing an enlargement of lysosomes and inhibiting functional delivery of proteins in the TGN (Bonay et al., 1996). Wild-type NOS2-GFP-transfected COS7 cells were treated with increasing concentrations of brefeldin A, monensin or megalomicin. Both brefeldin A and monensin drastically diminished the ·NO synthesis to 29 and 43% of the levels in the control at 10 μM respectively, whereas the addition of megalomicin produced only a small effect on NOS2 activity, which diminished to 70% of the control level (Fig. 6A). Curiously when we correlated these results with the incorporation of palmitic acid, BFA significantly inhibited the incorporation of [^{3}H]palmitate into NOS2 whereas the other two agents produced a limited effect on NOS2 palmitoylation. We also tested the effect of BFA on the myristoylated and palmitoylated NOS2 mutant. The data show that the palmitoylation of this mutant was insensitive to BFA (Fig. 6B). These results are consistent with the results obtained in the case of the doubly acylated p59^{fyn} in which palmitoylation is not affected by treatment with BFA (van't Hof and Resh, 1997). In consequence, drugs that affect the Golgi integrity, as well as the ER-to-Golgi transit or the Golgi-TGN progress, affect NOS2 activity. However, only BFA, when maintained throughout the entire radiolabeling process, drastically diminished palmitoylation of NOS2, rendering the most profound reduction in ·NO-synthesising activity.

The first 33 amino acids of NOS2 are not part of the catalytic core of the enzyme

Next, we wondered if the N-terminus of NOS2 might be involved in catalysis and if the changes detected in our mutant chimeras might arise from alterations in the three-dimensional folding of the protein. In addition, we also wanted to demonstrate whether, as in the case of NOS1 and NOS3, the N-terminus of NOS2 is involved in subcellular targeting. Hence, we created a deletion mutant of the first 33 amino acids of the recombinant NOS2 and expressed it in *E. coli*, a recombinant system with a simple post-translational mechanisms where we might bypass all the complex sorting machinery that mammalian cells possess. An additional advantage of *E. coli* as recombinant expression system for NOS is that the protein is inactive within the cell, because the bacteria lack tetrahydrobiopterin and calmodulin (Rodríguez-Crespo et al., 1996a). Very pure protein was obtained after purification by sequential affinity chromatography, first through the binding to a Ni^{2+}-NTA resin by means of the N-terminal polyHis tag and subsequently by binding to 2′,5′-ADP-Sepharose column through the C-terminal NADPH binding site (Fig. 7A). The absorbance spectrum was characterised by a high-spin peak at 394 nm in the presence of L-Arg and H_4B and flavin absorption maxima at ~460 and 485 nm; these are indistinguishable from that of the wild-type protein (Nishida and Ortiz de Montellano, 1998). In addition, whereas the boiled sample gave a clear monomeric (M) band with Coomassie Blue, a small amount of dimers (D) and monomers could be seen in the lane of the unboiled sample

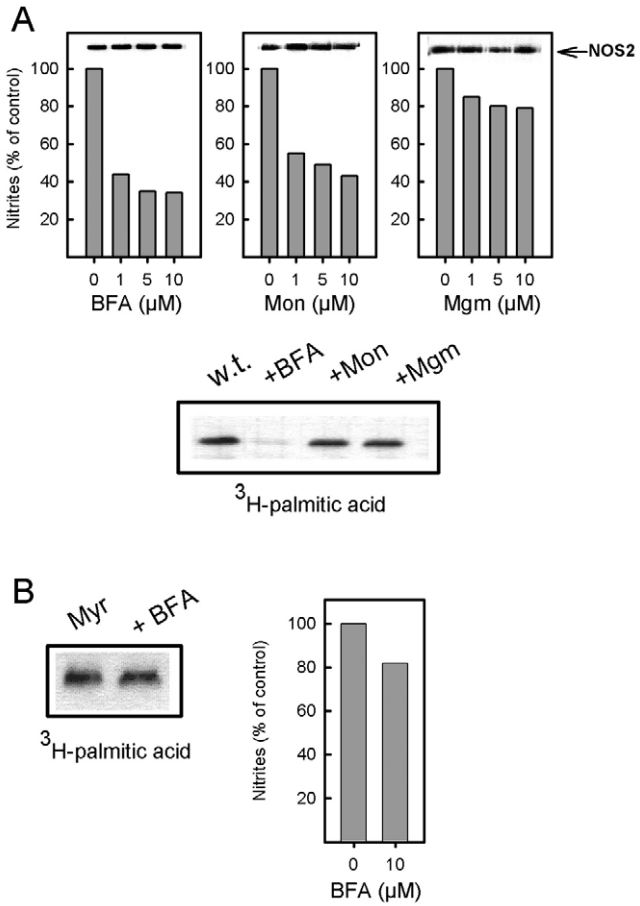

Fig. 6. Agents that disrupt the ER-to-Golgi traffic affect NOS2 activity and subcellular distribution. COS7 cells were transfected with the full-length wild-type (A) and Myr (B) NOS2-GFP chimeras and 12 hours later increasing concentrations of brefeldin, monensin or megalomicin were added to the cell culture for 16 hours. After the treatment, the NOS2 activity was determined with the Griess assay. In a parallel experiment, COS7 cells transfected with their (1-94) counterparts were incubated with or without the desired drug for 4 hours, then starved for 1 hour in DMEM without serum and were then metabolically labelled for 4 hours with [^{3}H]palmitic acid. Brefeldin A, monensin, megalomicin or DMSO (control) levels were maintained during the labelling period. The incorporation of radiolabelled palmitate was assessed both for wild-type NOS2(1-94)-GFP (A, bottom panel) and Myr NOS2(1-94) (B, left-hand panel, BFA only). The results shown are representative of two independent experiments.

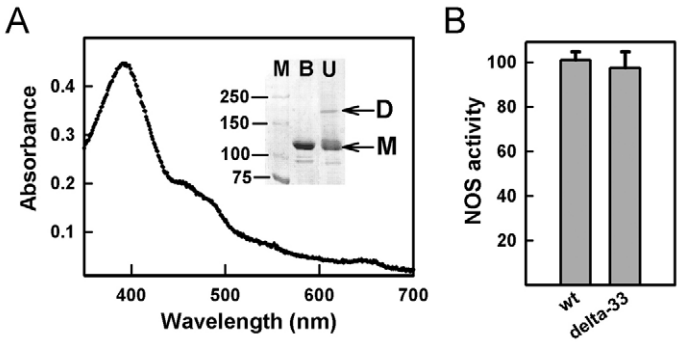

Fig. 7. Residues 1-33 of NOS2 are not part of the catalytic core of NOS2. (A) Absorbance spectrum of the recombinant NOS2 (Δ33) expressed in *E. coli*. The contribution of the heme prosthetic group is centered around 390 nm whereas the contribution of the FAD and FMN flavins is centered around 450 nm. The insert shows a Coomassie Blue-stained gel with molecular weight markers (M), boiled (B) NOS2 and unboiled (U) NOS2, where the SDS-resistant dimers (D) can be partially observed as distinct form the monomers (M). Approximately 2 μg of purified protein were loaded per lane. Panel B show the catalytic activity of the recombinant NOS2(Δ33) (delta-33) protein compared with the wild-type NOS2 (wt).

(Fig. 7A, insert). The presence of SDS-resistant dimers reflects the effective dimerisation of the sample in solution (Klatt et al., 1995). Although this mutant lacks the palmitoylation site and the neighbouring basic or hydrophobic amino acids (Pro 4 or Lys 6 and 10), it retains full catalytic activity compared with the recombinant NOS2 wild type (Fig. 7B). This result clearly establishes that the N-terminus of NOS2 (the first 33 amino acids) is dispensable for catalytic activity and is required for subcellular localisation when induced by cytokines or when transfected in mammalian cells.

Subcellular distribution of cytokine-induced NOS2 compared with the palmitoylated proteins PSD-95 and GAP-43

PSD-95 and GAP-43 are two well-characterised N-terminally palmitoylated proteins. Since treatment with cytokines induces the expression of NOS2 in multiple cell types we compared the subcellular distribution of endogenous NOS2 with transfected GAP-43 and PSD-95. When we transfected N-terminally palmitoylated wild-type PSD-95 and GAP-43 in COS7 cells we could observe immunofluorescence phenotypes that differed from that observed for the wild-type NOS2-GFP chimera (Fig. 8A). PSD-95-GFP displays a clear pattern of nuclear staining, a diffuse immunofluorescence along the cell cytoplasm and clear plasma membrane staining, whereas GAP-43 is absent from the cell nucleus, and distributes in patches in the cytoplasm in addition to the plasma membrane. In neither case could we observe the large perinuclear staining characteristic of Golgi network localisation that is observed in the case of wild-type NOS2-GFP. We can therefore conclude that the three N-terminally palmitoylated proteins differ in their subcellular distribution. In order to shed some light into the different staining patterns displayed by PSD-95 and NOS2 we transfected PSD-95-GFP in two cell lines in which inflammation can be induced with a mixture of cytokines and bacterial lipopolysaccharide, such as mouse C2C12 myotubes

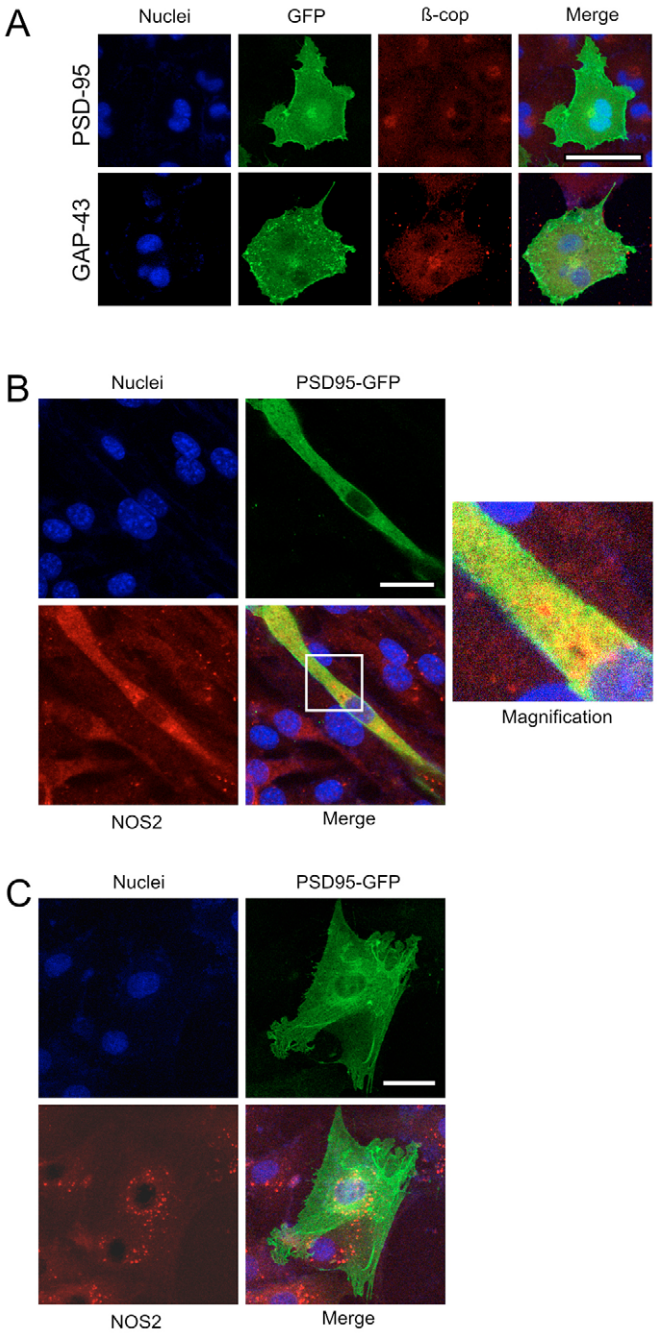

Fig. 8. The subcellular distribution of the palmitoylated proteins PSD-95, GAP-43 and NOS2 is different in COS7 cells, C2C12 myotubes and H9C2 cardiac myocytes. (A) Both PSD-95-GFP and GAP-43-GFP constructs were transfected in COS7 cells and the subcellular distribution was analysed with the Golgi marker β-cop labelled with a Cy3 secondary antibody (red). The right panels show the merges of the three fluorescence signals. Cell nuclei were stained with Hoechst 33258 (blue). (B) Mouse C2C12 myoblasts were converted into myotubes and a PSD-95 construct was transfected in the presence of a mixture of the cytokines LPS and IFN-γ that induce NOS2 expression. Inducible NOS is present to differing degrees in most of the cells with a patchy distribution (red staining). A magnified image of the boxed area in the merged image shows the colocalisation more clearly (right panel). (C) H9C2 rat cardiac myocytes were transfected with a PSD-95 construct in the presence of a mixture of the cytokines LPS and IFNγ that induce NOS2 expression. Bars, 50 μm.

and H9C2 cardiac myocytes. C2C12 myoblasts were converted into C2C12 myotubes and induction of NOS2 was achieved with a mixture of LPS and IFN-γ (Navarro-Lérida et al., 2004b) (Fig. 8B). When we transfected these myotubes with PSD-95-GFP, and compared their subcellular distribution with NOS2 stained with Cy3 (red), we could observe through laser confocal microscopy that most of the cells in the culture induced NOS2 expression which in turn displayed more particulate association with intracellular membranes and associated with perinuclear regions of the cell. Conversely, PSD-95-GFP could reach the plasma membrane and showed a more diffuse distribution along the cytoplasm (Fig. 8B, insert). Although there are certain areas of colocalisation, NOS2 displayed a patchy distribution that was not observed with PSD-95. Even larger differences were observed when NOS2 was induced in cardiac H9C2 myocytes and PSD-95-GFP was transfected (Fig. 8C). Most of the cells in culture expressed NOS2 (red Cy3 staining) that distributed in perinuclear secretory vesicles that irradiate from the nucleus. On the other hand, PSD-95-GFP stained the nucleus, the plasma membrane and distributed in fibre-like structures along the cytoplasm. In conclusion, the information conferred by the N-terminal palmitoylation of NOS2, PSD-95 and GAP-43 is not sufficient to dictate a similar pattern of distribution in subcellular compartments.

The non-palmitoylated C3S chimera is able to form dimers with the palmitoylated wild-type NOS2

Since our non-palmitoylated full-length C3S NOS2 chimera does not show enzymatic activity, we next investigated if palmitoylation of NOS2 mediates its ability to form dimers inside the cell. Using a commercial antibody that recognises the C-terminus of NOS2 together with an antibody that recognises GFP we could determine whether the (1-94)-GFP chimeras of the wild-type NOS2 and its C3S mutant can associate with the full-length NOS2 that is not tagged with GFP. When we used an anti-NOS2 antibody to immunoprecipitate the full-length NOS2 in association with the short chimeras cotransfected in the same cell we could precipitate both the wild-type protein as well as its non-palmitoylated counterpart (Fig. 9A, upper panel). When we performed the opposite experiment, that is immunoprecipitation of the GFP-tagged short chimeras with anti-GFP antibodies in cells cotransfected with non-tagged NOS2, we could retrieve the full-length wild-type NOS2 in association with the first 94 residues of both the wild-type NOS2 and the C3S mutant (Fig. 9, bottom panel). We could, therefore, conclude that the absence of activity of the C3S mutant is not due to its impaired dimerisation ability but rather to a defect in the subcellular traffic.

Discussion

The 3D structures of the heme domains of all three NOS have been obtained using recombinant protein preparations where the N-termini have been removed. In addition to facilitating crystallisation, it was assumed that these N-terminal extensions were involved in intracellular targeting of the enzymes. For instance, deletion of as many as 226 amino acids from the N-terminus of NOS1 produced a recombinant protein that maintained enzymatic activity at similar levels to its wild-type counterpart (Brenman et al., 1995). These first 226 residues

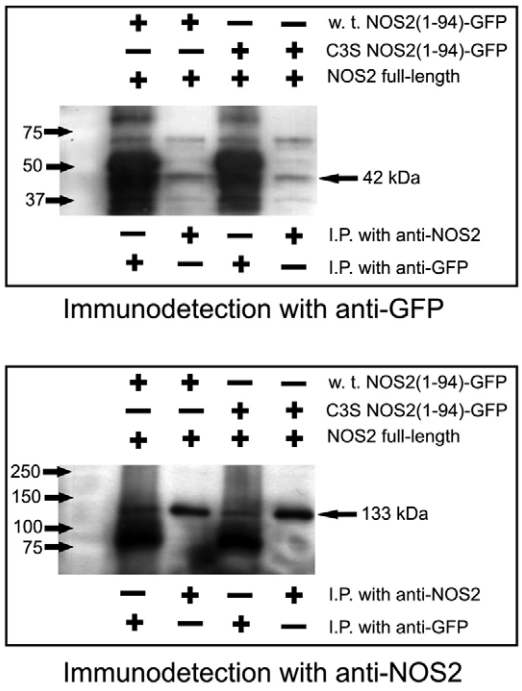

Fig. 9. The non-palmitoylated C3S is able to form dimers. COS7 cells were cotransfected with full-length NOS2 with either the wild-type or the C3S (1-94)-NOS2-GFP chimera. Antibodies that recognise the C-terminus of NOS2 or the GFP tag were used independently to immunoprecipitate the complexes. The immunodetection (western blot) was performed using both anti-GFP antibodies (upper panel) and anti-NOS2 antibodies (bottom panel). The (1-94) NOS2-GFP chimeras appear at 42 kDa whereas the NOS2 appears at 133 kDa.

contain a PDZ domain known to bind to numerous multi-PDZ proteins present at the post-synaptic region in neurons as well as to skeletal muscle syntrophin (Brenman et al., 1996). In the case of NOS3, there is abundant literature that establishes how the protein becomes N-terminally myristoylated and palmitoylated at Cys15 and Cys26 in a process required for caveolae targeting (Liu et al., 1996; Feron et al., 1998 and references therein). Somewhat unexpectedly, deletion of the first 52 residues of NOS3 renders a recombinant protein that retains the ability to form dimers as well as complete enzymatic activity (Rodríguez-Crespo et al., 1997). To the best of our knowledge, no N-terminal deletion studies have been performed on full-length NOS2, although as in the case of NOS1 and NOS3, the N-terminal end of the protein is probably involved in subcellular targeting. In fact, the crystal structure of the heme domain of NOS2 has been obtained after the deletion of 65 amino acids (Crane et al., 1998).

We have recently shown that after synthesis, NOS2 becomes palmitoylated at Cys3 and travels along the exocytic sorting route, partially reaching the plasma membrane (Navarro-Lérida et al., 2004a). With this in mind, we have created NOS2 chimeras fused to GFP and studied the mechanisms by which NOS2 progresses along the exocytic pathways. We have used complimentary techniques to demonstrate that: (1) palmitoylation of NOS2 determines its Golgi exit and its enzymatic activity; (2) myristoylation plus palmitoylation

leads to a chimera without increased enzymatic activity that reaches the plasma membrane within minutes in a process that is independent of the temperature; (3) a surrogate myristoylation site is unable to substitute for palmitoylation; (4) introduction of an additional palmitoylation site at Cys2 leads to caveolae targeting and probably to proteasomal degradation; (5) the N-terminus of NOS2 is not part of the catalytic part of the enzyme but rather an amino acid stretch where palmitoylation occurs as a mechanism of control of ·NO synthesis in vivo; (6) the amino acid sequence of NOS2, in conjunction with the N-terminal palmitoylation at Cys3 determines the subcellular localisation of the protein.

Since monomeric NOS2 is known to be inactive, our results indicate that after synthesis, NOS2 dimerises, palmitoylation allows the exit from the Golgi and the protein becomes active before reaching the plasma membrane. Our data suggest that the inactive, non-palmitoylated C3S mutant is able to form dimers although it becomes aggregated in the Golgi complex. Consequently, we found no clear correlation between palmitoylation and dimerisation, unlike the case of PSD-95 (Hsueh et al., 1997). In fact, when recombinantly expressed in *E. coli*, wild-type NOS2 is purified in its non-palmitoylated state (the bacteria lack palmitoyl transferase machinery) being active and dimeric (Nishida and Ortiz de Montellano, 1998).

By analogy with the neuronal proteins SNAP25 and GAP-43 (Gonzalo and Linder, 1998; Bijlmakers and Marsh, 2003), palmitoylation of NOS2 can be blocked by treatment with brefeldin A, but not by monensin or megalomicin. These two proteins are known to be located at axons but first accumulate at the TGN and are then transported bound to vesicles towards the plasma membrane. Hence, palmitoylation of NOS2 requires functional Golgi membranes either to be delivered to a specific location or, perhaps, to facilitate the palmitoylation reaction itself (Fig. 6). By contrast, both monensin and megalomicin also affect NOS2-mediated ·NO synthesis, albeit to a different extent to brefeldin A. Thus, alterations in the sorting route of NOS2 in the Golgi-TGN machinery also have implications for activity. Our observation that brefeldin A is unable to abrogate palmitoylation of the Myr mutant clearly reinforces the idea that myristoylation conveys an alternative route of sorting on wild-type NOS2, which differs from that followed by the wild-type polypeptide.

In the case of endothelial NOS3, the purified recombinant nonpalmitoylated mutant is catalytically indistinguishable from the wild-type enzyme, but produces less ·NO in stimulated cells (Liu et al., 1996). Likewise, we have created a deletional NOS2 in which we have removed the palmitoylatable Cys as well as the neighbouring residues. When expressed in *E. coli*, this enzyme synthesises ·NO at similar levels than the wild-type recombinant protein. Hence, as in the case of NOS1 and NOS3, we have demonstrated here that the N-terminus is not part of the catalytical core of the enzyme. The absence of activity observed in the case of the C3S mutant, together with its increased proteolysis (Navarro-Lérida et al., 2004a) must correlate with the cellular quality control machinery, which recognises the inability of this construct to progress along the sorting pathway and probably targets it for degradation.

We also observed clear differences in the subcellular distribution of NOS2 when compared with GAP-43 and PSD-95, two other N-terminally palmitoylated polypeptides (Fig. 8). We correlate these differences with the dissimilar amino acid sequences of these proteins as well as with the interaction with other cellular proteins. In fact, our wild-type NOS2 is not enriched in caveolae and even the non-palmitoylated C3S-C5S double mutant of PSD-95 can be targeted to rafts/caveolae (Perez and Bredt, 1998). Considering that NOS2 is synthesised in multiple cell types that are polarised (i.e. hepatocytes, epithelial cells, neurons) it is conceivable that palmitoylation of NOS2 also acts as a targeting signal for vectorial ·NO synthesis in certain tissues. Similarly, palmitoylation of PSD-95 together with a specific N-terminal amino acid sequence mediates its traffic with vesiculotubular structures to dendritic clusters in hippocampal neurons but also to the basolateral membrane of polarised epithelial cells (El-Husseini et al., 2000; Christopherson et al., 2003). In this particular case, the PDZ domains of PSD-95 determines the subcellular positioning of the protein together with the signals conveyed by the palmitoylation motif, both of them being indispensable for the correct targeting of PSD-95. We suspect that a similar situation is occurring in the case of NOS2, in which the concerted action of palmitoylated plus certain protein-protein interactions dictates the subcellular localisation. At this point we must comment on the fact that 70 N-terminal amino acids of NOS2 are known to interact with the membrane protein NAP110 (a protein of unknown function) as well as with kalirin (Ratovitski et al., 1999a; Ratovitski et al., 1999b). Since it is not established how NOS2 interacts with these two polypeptides during its sorting as well as the functional significance of these interactions, it remains to be confirmed how palmitoylation would affect binding to these two proteins. It is then plausible that palmitoylation enables the interaction of NOS2 with either kalirin or NAP-110.

Materials and Methods

Materials

The source of most of the materials has been described before (Navarro-Lérida et al., 2004a; Navarro-Lérida et al., 2004b). L-Arginine and tetrahydrobiopterin were obtained from Merck. Diaminorhodamine-4M (DAR-4M) was purchased from Calbiochem. Megalomicin was a generous gift from Balbino Alarcón (Universidad Autónoma de Madrid, Madrid, Spain).

Construction of the GFP fusion proteins, plasmids and mutagenesis

We have described the cloning and expression of the full-length wild-type NOS2, which possessed the initial sequence MACPWKFLFKVKSYQSD. Site-directed mutagenesis was used to introduce the desired mutations and we created the following constructs: wild-type, C3S, Myr, Myr/C3S, A2C (Fig. 1). Every mutant was obtained as a full-length NOS2-GFP chimera and as a NOS2-(1-94)-GFP chimera. The restriction sites used are described in detail elsewhere (Navarro-Lérida et al., 2004a; Navarro-Lérida et al., 2004b). The wild-type GAP-43-GFP and the PSD-95-GFP clones were generous gifts of Luc Berthiaume (University of Alberta, Alberta, Canada) and David Bredt (University of California, San Francisco, CA).

Immunoblot analysis, cellular fractionation, laser confocal microscopy, metabolic labelling and immunoprecipitation

The cellular biology techniques described in this manuscript were performed as described elsewhere (Navarro-Lérida et al., 2004a; Navarro-Lérida et al., 2004b).

Fluorescence recovery after photobleaching

To study the dynamics of NOS2 and its myristoylated mutant in living cells, we used fluorescence recovery after photobleaching (FRAP). Focusing 100% of argon laser power (blue light of 488-nm length) on small areas of plasma membrane, NOS2 associated in this region was photobleached irreversibly for 50 seconds. Then, 3% of laser power was used to image the GFP at different times. The changes in the signal intensity before photobleaching and in the subsequent time points after photobleaching were analysed.

Preparation of caveolin-enriched DRMs

Our flotation experiments in the presence of Triton X-100 followed the published protocol of Lisanti (Lisanti et al., 1999). The method is described in detail elsewhere (Navarro-Lérida et al., 2004a; Navarro-Lérida et al., 2004b).

Recombinant expression of NOS in *E. coli*, purification and NOS2 assay

The cDNA coding for NOS2 with an N-terminal deletion of the first 33 amino acids was constructed by PCR with a *Nde*I site at the 5′ end, subcloned in the pGEMT vector (Promega) and sequenced. The amplified band was digested with *Nde*I and *Xba*I, cloned in the corresponding sites of the expression vector pCWori and was named Δ33-NOS2. This construction was used to routinely transform competent BL21 cells (Novagen) where the coexpression vector for calmodulin was already inserted. Four litres of 2×YT media were used for protein expression at 22°C. The protein was purified using two affinity columns as previously described (Rodríguez-Crespo et al., 1996a; Rodríguez-Crespo et al., 1996b). The NOS assay has been described elsewhere (Navarro-Lérida et al., 2004a; Navarro-Lérida et al., 2004b).

References

Bijlmakers, M. J. and Marsh, M. (2003). The on-off story of protein palmitoylation. *Trends Cell Biol.* **13**, 32-42.

Bonay, P., Munro, S., Fresno, M. and Alarcon, B. (1996). Intra-Golgi transport inhibition by megalomicin. *J. Biol. Chem.* **271**, 3719-3726.

Brenman, J. E., Chao, D. S., Xia, H., Aldape, K. and Bredt, D. S. (1995). Nitric oxide synthase complexed with dystrophin and absent from skeletal muscle sarcolemma in Duchenne muscular dystrophy. *Cell* **82**, 743-752.

Brenman, J. E., Chao, D. S., Gee, S. H., McGee, A. W., Craven, S. E., Santillano, D. R., Wu, Z., Huang, F., Xia, H., Peters, M. F. et al. (1996). Interaction of nitric oxide synthase with the postsynaptic density protein PSD-95 and alpha1-syntrophin mediated by PDZ domains. *Cell* **84**, 757-767.

Casey, P. J. (1995). Protein lipidation in cell signaling. *Science* **268**, 221-225.

Christopherson, K. S., Sweeney, N. T., Craven, S. E., Kang, R., El-Husseini, A. E. and Bredt, D. S. (2003). Lipid- and protein-mediated multimerization of PSD-95: implications for receptor clustering and assembly of synaptic protein networks. *J. Cell Sci.* **116**, 3213-3219.

Crane, B. R., Arvai, A. S., Ghosh, D. K., Wu, C., Getzoff, E. D., Stuehr, D. J. and Tainer, J. A. (1998). Structure of nitric oxide synthase oxygenase dimer with pterin and substrate. *Science* **279**, 2121-2126.

Dietrich, L. E. and Ungermann, C. (2004). On the mechanism of protein palmitoylation. *EMBO Rep.* **5**, 1053-1057.

Dunphy, J. T. and Linder, M. E. (1998). Signalling functions of protein palmitoylation. *Biochim. Biophys. Acta* **1436**, 245-261.

Dunphy, J. T., Greentree, W. K., Manahan, C. L. and Linder, M. E. (1996). G-protein palmitoyltransferase activity is enriched in plasma membranes. *J. Biol. Chem.* **271**, 7154-7159.

El-Husseini, A. E., Craven, S. E., Chetkovich, D. M., Firestein, B. L., Schnell, E., Aoki, C. and Bredt, D. S. (2000). Dual palmitoylation of PSD-95 mediates its vesiculotubular sorting, postsynaptic targeting, and ion channel clustering. *J. Cell Biol.* **148**, 159-172.

Felley-Bosco, E., Bender, F. C., Courjault-Gautier, F., Bron, C. and Quest, A. F. (2000). Caveolin-1 down-regulates inducible nitric oxide synthase via the proteasome pathway in human colon carcinoma cells. *Proc. Natl. Acad. Sci. USA* **97**, 14334-14339.

Feron, O., Saldana, F., Michel, J. B. and Michel, T. (1998). The endothelial nitric-oxide synthase-caveolin regulatory cycle. *J. Biol. Chem.* **273**, 3125-3128.

García-Cardena, G., Martasek, P., Masters, B. S., Skidd, P. M., Couet, J., Li, S., Lisanti, M. P. and Sessa, W. C. (1997). Dissecting the interaction between nitric oxide synthase (NOS) and caveolin. Functional significance of the nos caveolin binding domain in vivo. *J. Biol. Chem.* **272**, 25437-25440.

Gonzalo, S. and Linder, M. E. (1998). SNAP-25 palmitoylation and plasma membrane targeting require a functional secretory pathway. *Mol. Biol. Cell* **9**, 585-597.

Griffiths, G., Quinn, P. and Warren, G. (1983). Dissection of the Golgi complex. I. Monensin inhibits the transport of viral membrane proteins from medial to trans Golgi cisternae in baby hamster kidney cells infected with Semliki Forest virus. *J. Cell Biol.* **96**, 835-850.

Gubitosi-Klug, R. A., Mancuso, D. J. and Gross, R. W. (2005). The human Kv1.1 channel is palmitoylated, modulating voltage sensing: Identification of a palmitoylation consensus sequence. *Proc. Natl. Acad. Sci. USA* **102**, 5964-5968.

Hess, D. T., Patterson, S. I., Smith, D. S. and Skene, J. H. (1993). Neuronal growth cone collapse and inhibition of protein fatty acylation by nitric oxide. *Nature* **366**, 562-565.

Hsueh, Y. P., Kim, E. and Sheng, M. (1997). Disulfide-linked head-to-head multimerization in the mechanism of ion channel clustering by PSD-95. *Neuron* **18**, 803-814.

James, G. and Olson, E. N. (1990). Fatty acylated proteins as components of intracellular signaling pathways. *Biochemistry* **29**, 2623-2634.

Klatt, P., Schmidt, K., Lehner, D., Glatter, O., Bachinger, H. P. and Mayer, B. (1995). Structural analysis of porcine brain nitric oxide synthase reveals a role for tetrahydrobiopterin and L-arginine in the formation of an SDS-resistant dimer. *EMBO J.* **14**, 3687-3695.

Klausner, R. D., Donaldson, J. G. and Lippincott-Schwartz, J. (1992). Brefeldin A: insights into the control of membrane traffic and organelle structure. *J. Cell Biol.* **116**, 1071-1080.

Lisanti, M. P., Sargiacomo, M. and Scherer, P. E. (1999). Purification of caveolae-derived membrane microdomains containing lipid-anchored signaling molecules, such as GPI-anchored proteins, H-Ras, Src-family tyrosine kinases, eNOS, and G-protein alpha-, beta-, and gamma-subunits. *Methods Mol. Biol.* **116**, 51-60.

Liu, J., Garcia-Cardena, G. and Sessa, W. C. (1996). Palmitoylation of endothelial nitric oxide synthase is necessary for optimal stimulated release of nitric oxide: implications for caveolae localization. *Biochemistry* **35**, 13277-13281.

Liu, J., Hughes, T. E. and Sessa, W. C. (1997). The first 35 amino acids and fatty acylation sites determine the molecular targeting of endothelial nitric oxide synthase into the Golgi region of cells: a green fluorescent protein study. *J. Cell Biol.* **137**, 1525-1535.

Magee, A. I. and Seabra, M. C. (2003). Are prenyl groups on proteins sticky fingers or greasy handles? *Biochem. J.* **376**, e3-e4.

McCabe, J. B. and Berthiaume, L. G. (2001). N-terminal protein acylation confers localization to cholesterol, sphingolipid-enriched membranes but not to lipid rafts/caveolae. *Mol. Biol. Cell* **12**, 3601-3617.

Milligan, G., Parenti, M. and Magee, A. I. (1995). The dynamic role of palmitoylation in signal transduction. *Trends Biochem. Sci.* **20**, 181-187.

Navarro-Lérida, I., Alvarez-Barrientos, A., Gavilanes, F. and Rodríguez-Crespo, I. (2002). Distance-dependent cellular palmitoylation of de-novo-designed sequences and their translocation to plasma membrane subdomains. *J. Cell Sci.* **115**, 3119-3130.

Navarro-Lérida, I., Corvi, M. M., Alvarez-Barrientos, A., Gavilanes, F., Berthiaume, L. G. and Rodríguez-Crespo, I. (2004a). Palmitoylation of inducible nitric-oxide synthase at Cys-3 is required for proper intracellular traffic and nitric oxide synthesis. *J. Biol. Chem.* **279**, 55682-55689.

Navarro-Lérida, I., Portoles, M. T., Alvarez-Barrientos, A., Gavilanes, F., Bosca, L. and Rodríguez-Crespo, I. (2004b). Induction of nitric oxide synthase-2 proceeds with the concomitant downregulation of the endogenous caveolin levels. *J. Cell Sci.* **117**, 1687-1697.

Nishida, C. R. and Ortiz de Montellano, P. R. (1998). Electron transfer and catalytic activity of nitric oxide synthases. Chimeric constructs of the neuronal, inducible, and endothelial isoforms. *J. Biol. Chem.* **273**, 5566-5571.

Perez, A. S. and Bredt, D. S. (1998). The N-terminal PDZ-containing region of postsynaptic density-95 mediates association with caveolar-like lipid domains. *Neurosci. Lett.* **258**, 121-123.

Ratovitski, E. A., Bao, C., Quick, R. A., McMillan, A., Kozlovsky, C. and Lowenstein, C. J. (1999a). An inducible nitric-oxide synthase (NOS)-associated protein inhibits NOS dimerization and activity. *J. Biol. Chem.* **274**, 30250-30257.

Ratovitski, E. A., Alam, M. R., Quick, R. A., McMillan, A., Bao, C., Kozlovsky, C., Hand, T. A., Johnson, R. C., Mains, R. E., Eipper, B. A. et al. (1999b). Kalirin inhibition of inducible nitric-oxide synthase. *J. Biol. Chem.* **274**, 993-999.

Resh, M. D. (1999). Fatty acylation of proteins: new insights into membrane targeting of myristoylated and palmitoylated proteins. *Biochim. Biophys. Acta* **1451**, 1-16.

Rodríguez-Crespo, I., Gerber, N. C. and Ortiz de Montellano, P. R. (1996a). Endothelial nitric-oxide synthase. Expression in Escherichia coli, spectroscopic characterization, and role of tetrahydrobiopterin in dimer formation. *J. Biol. Chem.* **271**, 11462-11467.

Rodríguez-Crespo, I. and Ortiz de Montellano, P. R. (1996b). Human endothelial nitric oxide synthase: expression in Escherichia coli, coexpression with calmodulin, and characterization. *Arch. Biochem. Biophys.* **336**, 151-156.

Rodríguez-Crespo, I., Moenne-Loccoz, P., Loehr, T. M. and Ortiz de Montellano, P. R. (1997). Endothelial nitric oxide synthase: modulations of the distal heme site produced by progressive N-terminal deletions. *Biochemistry* **36**, 8530-8538.

Rothman, J. E. and Orci, L. (1992). Molecular dissection of the secretory pathway. *Nature* **355**, 409-415.

Smotrys, J. E. and Linder, M. E. (2004). Palmitoylation of intracellular signaling proteins: regulation and function. *Annu. Rev. Biochem.* **73**, 559-587.

van't Hof, W. and Resh, M. D. (1997). Rapid plasma membrane anchoring of newly synthesized p59fyn: selective requirement for NH2-terminal myristoylation and palmitoylation at cysteine-3. *J. Cell Biol.* **136**, 1023-1035.

Zhang, F. L. and Casey, P. J. (1996). Protein prenylation: molecular mechanisms and functional consequences. *Annu. Rev. Biochem.* **65**, 241-269.